ELSEVIER

www.elsevier.com/locate/ica
Inorganica Chimica Acta 326 (2001) 53–64

Inorganica Chimica Acta

The $[Cu_2(O_2CMe)_4(btd)_2]$ complex as a bridging unit: preparation, characterisation, X-ray structure and magnetism of the 2D coordination polymer $\{[Cu_6(O_2CMe)_8(OMe)_4(btd)_2]\}_n$ (btd = 2,1,3-benzothiadiazole)

Konstantina Skorda [a], Giannis S. Papaefstathiou [a], Anastasios Vafiadis [b], Alexandra Lithoxoidou [b], Catherine P. Raptopoulou [c], Aris Terzis [c], Vassilis Psycharis [c], Evangelos Bakalbassis [b,*], Vassilis Tangoulis [d,*], Spyros P. Perlepes [a,*]

[a] *Laboratory of Inorganic Chemistry, Department of Chemistry, University of Patras, 26504 Patras, Greece*
[b] *Department of Chemistry, Aristotle University of Thessaloniki, 54006 Thessaloniki, Greece*
[c] *Institute of Materials Science, NCSR "Demokritos", 15310 Aghia Paraskevi Attikis, Greece*
[d] *Department of Materials Science, University of Patras, 26504 Patras, Greece*

Received 8 June 2001; accepted 27 July 2001

In dedication to the late Professor Olivier Kahn, one of the pioneers of molecular magnetism

Abstract

A systematic investigation of the $[Cu_2(O_2CMe)_4(H_2O)_2]$/btd reaction system is described, where btd = 2,1,3-benzothiadiazole. Reaction of $[Cu_2(O_2CMe)_4(H_2O)_2]$ with 5–8 equiv. of btd in both MeCN and MeOH yields $[Cu_2(O_2CMe)_4(btd)_2]$ (**1**) in 40–50% yields. Treatment of $[Cu_2(O_2CMe)_4(H_2O)_2]$ with 1.4 or 0.7 equiv. of btd in MeOH leads to the precipitation of the polymeric compound $\{[Cu_6(O_2CMe)_8(OMe)_4(btd)_2]\}$ (**2**) in 82% yield. Reaction of **1** with two equivalents of $[Cu_2(O_2CMe)_4(H_2O)_2]$ in MeOH under reflux provides an additional route to **2**. The structure of **1** consists of centrosymmetric dinuclear $[Cu_2(O_2CMe)_4(btd)_2]$ molecules of the paddle-wheel cage type. The two Cu^{II} ions are bridged by four $\eta^1{:}\eta^1{:}\mu_2$ acetates, while a monodentate btd is at the apex of the square pyramid of each metal centre. The 2D structure of **2** consists of chains of tetranuclear, planar $Cu_4(OMe)_4(O_2CMe)_4$ repeating units running along the *a* axis, which are connected along the cell body diagonal via $Cu_2(O_2CMe)_4(btd)_2$ paddle-wheel dinuclear units. The btd molecules behave as bidentate bridging ligands. Within the tetranuclear units, each Cu^{II} ion is connected via two acetate bridges with one neighbouring Cu^{II} ion and via two methoxo bridges with the other neighbouring Cu^{II} ion; intertetranuclear linking is provided by two monoatomic acetate bridges. The results of solid state magnetic susceptibility studies are described for complex **2** in the temperature range 3–300 K. The results reveal antiferromagnetic exchange interactions between the Cu^{II} ions. The complicated structure of **2** does not permit an exact treatment for the determination of the various exchange interactions. However, an approximate 3-*J* magnetic model was constructed, resulting in an excellent fit. An orbital interpretation of the *J*-trend derived is also attempted.

Keywords: Acetate complexes; 2,1,3-Benzothiadiazole complexes; Copper(II) complexes; EPR spectra; Magnetic properties; Two-dimensional coordination polymers

1. Introduction

Our groups are involved in the preparation and characterization of transition metal complexes [1] that present interest in the frame of molecular magnetism, which is a new branch of science [2]. Magnetic materials prepared from molecules, not atoms or ions, have

* Corresponding authors. Tel.: +30-61-997 146; fax: +30-61-997 118.
E-mail address: perlepes@patreas.upatras.gr (S.P. Perlepes).

0020-1693/01/$ - see front matter
PII: S0020-1693(01)00594-1

enabled the establishment of a diverse new class of magnets with magnetic ordering temperatures well above room temperature [3]. As a class, molecule-based magnets are anticipated to exhibit a variety of technologically important features that include modulation of properties via organic and coordination chemistry methodologies, compatibility with polymers for composites, low density, transparency, low temperature processibility, insulation, solubility, high coercivity (''hard'' magnets), low environmental contamination, biocompatibility, high permeability, high magnetization, low magnetic anisotropy, semiconducting behaviour, etc. Many of these characteristics are not available with conventional atom-based magnets.

From the chemical point of view, the two main families of coordination compounds that are the subject of molecular magnetism comprise: (a) coordination polymers (mainly three-dimensional, 3D) that are molecule-based magnets [4], i.e. molecular compounds exhibiting a spontaneous magnetization below a critical temperature, T_c, and (b) high-spin clusters, i.e. large molecules or ions which have the ability to function as magnetisable magnets below a critical (blocking) temperature, owing to intrinsic intramolecular properties than intermolecular interactions and long-range ordering [5].

Restricting further discussion to polymeric molecule-based magnets, we can mention that these compounds may contain the same metal ion, two kinds of spin carriers (either two different metal ions or a metal ion and an organic radical) and, in a very limited number of cases, three spin carriers. The attainment of magnetic ordering generally requires the organization of transition metal centres into 3D networks [6]. However, to better interpret magnetic properties of complex 3D solids, reduced dimensionalities, i.e. 1D and 2D are preferred to develop the necessary theoretical models [7].

Bidentate bridging *N*,*N*′-donor ligands have been extensively used in the last 10 years [7,8] with the aim of obtaining polymeric frameworks having potential properties in different areas of material science, such as electrical conductivity [9], magnetism [4,7], photomechanical behaviour [10], clathration ability and catalysis [11]. They are best classified according to the disposition of their lone pairs [12], which varies from linear (bridging angles 180°; e.g. pyrazine and 4,4′-bipyridine) through obtuse (bridging angle 120°; e.g. pyrimidine) and acute (bridging angle 60°; e.g. pyridazine) to parallel (bridging angle 0°; e.g. 1,8-naphthyridine). The type of the bridging ligand has immense influence on the nature of the coordination framework adopted.

One of the less explored non-linear bidentate bridging *N*,*N*′-donors is 2,1,3-benzothiadiazole (btd). This molecule is considered to be a potential ligand for construction of honeycomb and graphite-like structures [13]. We recently reported the employment of btd to construct the 2D arrays $\{[CuCl(btd)]\}_n$ [14], $\{[CuCl_2(btd)]\}_n$ [14] and $\{[CoX_2(btd)]\}_n$ [15], where X = Cl, Br. The cobalt(II) and copper(II) complexes consist of $\{[M(\mu\text{-}X)_2]\}_n$ linear chains running along the *a* axis linked via btd bridges along the *b* axis. In the copper(I) complex, within each layer the metal ions are bridged by two chloro ligands and two btd molecules. The columns of stacked btd molecules present in the crystal structure of the free ligand [16] are maintained in the lattices of the complexes. The magnetic properties of both cobalt(II) complexes were explained [15] by the presence of a very weak ferromagnetic intrachain Co···Co exchange interaction through the $(\mu\text{-}X)_2$ bridges and a moderate antiferromagnetic Co···Co interaction through the μ-btd ligands. More recently, our efforts have turned toward the use of coligands other than halides in order to see how they might affect the structures and magnetic properties of the products. The first non-halide ligand of our choice has been the acetate ion. In this report, we describe the identity and magnetic characterization of the products obtained from the $[Cu_2(O_2CMe)_4(H_2O)_2]$/btd reaction system.

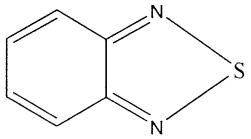

btd

2. Experimental

2.1. Reagents and physical measurements

All manipulations were performed under aerobic conditions. All chemicals and solvents were purchased from commercial sources and used without further purification. Microanalyses (C, H and N) were performed by the University of Ioannina Microanalytical Laboratory using an EA 1108 Carlo Erba analyzer. Copper(II) was estimated gravimetrically as copper(II) quinaldate [17]. IR spectra (4000–450 cm^{-1}) were recorded on a Perkin–Elmer 16 PC spectrometer with samples prepared as KBr pellets. Magnetic susceptibility measurements were carried out on a polycrystalline sample of complex **2** (see below) in the 3–300 K range under a magnetic field of 6000 G using a Quantum Design SQUID susceptometer. The experimental magnetic susceptibilities were corrected for the diamagnetic response using Pascal's constants. Solid-state EPR spectra at 4 and 300 K were recorded on a Bruker ER 200D-SRC X-band spectrometer, equipped with an Ox-

ford ESR 9 helium continuous-flow cryostat, a Hall probe and a Hewlett–Packard frequency meter.

2.2. Preparation of $[Cu_2(O_2CMe)_4(btd)_2]$ (1)

Solid $[Cu_2(O_2CMe)_4(H_2O)_2]$ (0.12 g, 0.3 mmol) was slowly dissolved with stirring in a solution of btd (0.33 g, 2.4 mmol) in MeCN (100 ml). A blue–green homogeneous solution was obtained. This was allowed to concentrate by evaporation at room temperature to give green crystals (some were suitable for single-crystal X-ray crystallography) of the product. The crystals were collected by filtration, washed with Et_2O and dried in air. Yield: 0.09 g (47% based on the metal salt). *Anal.* Calc. for $C_{20}H_{20}N_4Cu_2O_8S_2$: C, 37.79; H, 3.18; N, 8.82; Cu, 19.99. Found: C, 38.01; H, 3.25; N, 8.94; Cu, 19.27%. Selected IR spectral data (cm^{-1}): 1554 sb, 1438 m, 1404 m, 1338 w, 920 w, 830 w, 676 m, 566 w.

Table 1
Crystallographic data for complexes **1** and **2**

	1	**2**
Empirical formula	$C_{20}H_{20}N_4Cu_2O_8S_2$	$C_{16}H_{22}N_2Cu_3O_{10}S$ [a]
Formula weight	635.60	625.04
Crystal dimensions (mm)	$0.15\times0.35\times0.40$	$0.20\times0.30\times0.50$
Crystal system	triclinic	triclinic
Space group	$P\bar{1}$	$P\bar{1}$
a (Å)	7.846(1)	7.628(4)
b (Å)	7.889(1)	8.953(4)
c (Å)	10.764(2)	17.197(8)
α (°)	75.98(1)	91.34(1)
β (°)	72.81(1)	100.65(2)
γ (°)	86.61(1)	99.31(2)
V (Å^3)	617.5(2)	1137.3(9)
Z	1	2
D_{calc} (g cm^{-3})	1.709	1.825
$F(000)$	322	630
μ (mm^{-1})	1.944	2.925
λ(Mo Kα) (Å)	0.71070	0.71073
Temperature	298	298
Scan mode	θ–2θ	θ–2θ
Scan speed (° min^{-1})	3.0	3.3
Scan range (°)	$2.5+\alpha_1\alpha_2$ separation	$2.4+\alpha_1\alpha_2$ separation
θ range (°)	2.9–25.0	2.3–25.0
Reflections collected	2307	4145
Independent reflections (R_{int})	2138 (0.0168)	4001 (0.0192)
Range of h	−9 to 9	−8 to 9
Range of k	0 to 9	−10 to 10
Range of l	−12 to 12	−20 to 0
Number of refined parameters	203	369
Observed reflections [$I>2\sigma(I)$]	2021	3599
Final R_1 [b], wR_2 [c] [$I>2\sigma(I)$]	0.0275, 0.0774	0.0264, 0.0714
Goodness-of-fit (on F^2)	1.109	1.053

[a] This is the crystallographic formula, i.e. $Cu_3(O_2CMe)_4(OMe)_2(btd)$; however, the chemical formula used throughout the paper is $\{[Cu_6(O_2CMe)_8(OMe)_4(btd)_2]\}_n$ because it shows more clearly that the structure consists of dinuclear and tetranuclear units.

[b] $R_1=\Sigma(|F_o|-|F_c|)/\Sigma(|F_o|)$.

[c] $wR_2=\{\Sigma[w(F_o^2-F_c^2)^2]/\Sigma[w(F_o^2)^2]\}^{1/2}$, where $w=1/[\sigma^2(F_o^2)+(0.0330P)^2+(0.2934P)]$ for **1** and $w=1/[\sigma^2(F_o^2)+(0.0294P)^2+(0.5078P)]$ for **2** with $P=(\max(F_o^2,0)+2F_c^2)/3$.

2.3. Preparation of $\{[Cu_6(O_2CMe)_8(OMe)_4(btd)_2]\}_n$ (2)

2.3.1. Method A

To a solution of $[Cu_2(O_2CMe)_4(H_2O)_2]$ (0.20 g, 0.5 mmol) in MeOH (40 ml) was added a solution of btd (0.10 g, 0.7 mmol) in the same solvent. The green solution obtained was stirred at ambient temperature for 30 min and allowed to stand undisturbed for 2 weeks. Well-formed, X-ray quality crystals of the product slowly appeared. The green prismatic crystals were collected by filtration, washed with cold MeOH and Et_2O and dried in air. Yield: 0.17 g (82% based on copper). *Anal.* Calc. for $C_{16}H_{22}N_2Cu_3O_{10}S$: C, 30.74; H, 3.55; N, 4.48; Cu, 30.50. Found: C, 30.45; H, 3.61; N, 4.52; Cu, 29.87%. Selected IR spectral data (cm^{-1}): 1595 sh, 1576 sb, 1455 sh, 1426 s, 1342 w, 1024 m, 914 w, 864 w, 760 w, 682 m, 570 w.

2.3.2. Method B

Solid complex **1** (0.19 g, 0.3 mmol) was dissolved in a stirred blue–green solution of $[Cu_2(O_2CMe)_4(H_2O)_2]$ (0.24 g, 0.6 mmol) in MeOH (70 ml) under reflux. The reflux was continued for a further 30 min. The reaction mixture was filtered to remove a small quantity of a blue powder and the resulting green solution was layered with Et_2O (60 ml). Slow mixing yielded green crystals of **2**, which were collected by filtration, washed with cold MeOH and Et_2O, and dried in air. Yields as high as 70% were obtained. The identity of the product was confirmed by elemental analyses and IR spectroscopic comparison with samples from method A.

2.4. X-ray crystallography

Data collection, crystal data and structure solution information are listed in Table 1. Crystals of **1** and **2** were mounted in air. Diffraction measurements were made on a $P2_1$ Nicolet diffractometer upgraded by Crystal Logic using Zr-filtered Mo radiation (**1**) and on a Crystal Logic Dual Goniometer diffractometer using graphite-monochromated Mo radiation (**2**). Unit cell dimensions were determined and refined by using the angular settings of 25 automatically centred reflections in the range $11<2\theta<23°$. Three standard reflections monitored every 97 reflections showed less than 3% variation and no decay. Lorentz polarization and Ψ-scan absorption correction were applied using Crystal Logic software.

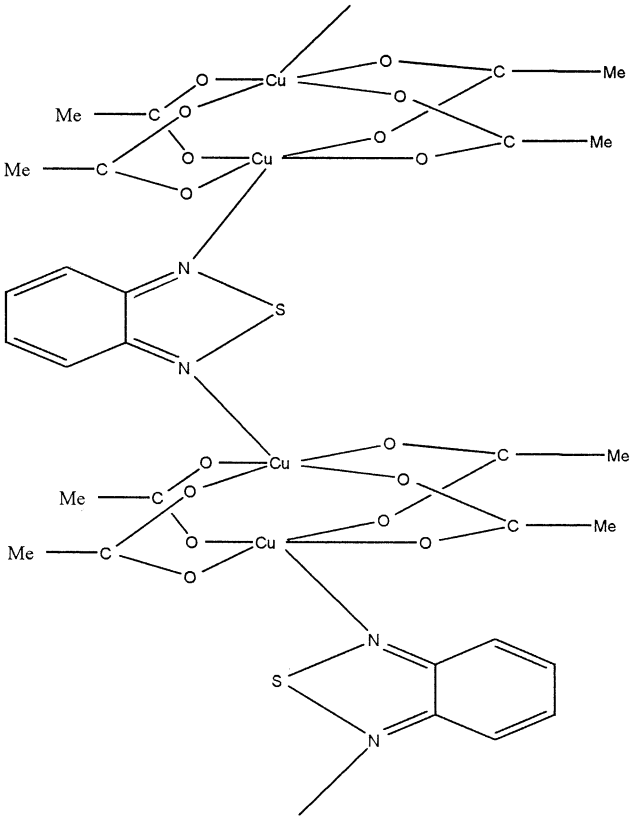

Fig. 1. The proposed one-dimensional zigzag structure obtained from the 1:1 reaction between $[Cu_2(O_2CMe)_4(btd)_2]$ and btd (see text).

The structures were solved by direct methods using SHELXS-86 [18] and refined by full-matrix least-squares techniques on F^2 with SHELXL-93 [19]. For both structures all non-H atoms were refined with anisotropic thermal parameters. All H atoms [except those of C(15) in **2** which were introduced at calculated position as riding on their bonded atom] were located by difference maps and refined isotropically. The maximum and minimum residual peaks in the final difference map were 0.426, -0.328 e Å^{-3} for **1** and 0.403, -0.447 e Å^{-3} for **2**. The largest shift/e.s.d. values in the final cycle were 0.022 (**1**) and 0.049 (**2**).

3. Results and discussion

3.1. Syntheses

The initial reaction explored was that between $[Cu_2(O_2CMe)_4(H_2O)_2]$ and 1 equiv. of btd in MeCN. This solvent facilitates a rapid reaction, a colour change to green and the subsequent precipitation of a green powder. Analytical data are consistent with the formulation $Cu_2(O_2CMe)_4(btd)$ expected for a $\{–Cu_2(O_2CMe)_4–btd– Cu_2(O_2CMe)_4–btd–\}_n$ chain polymer. Use of very dilute solutions yielded microcrystals, but, unfortunately, numerous attempts to obtain crystals suitable for crystallographic studies all proved in vain. An initial indication that the product may be polymeric is the very low solubility in solvents with which it does not react. The IR spectrum of the green powder exhibits the IR antisymmetric and symmetric carboxylate stretching vibrations at 1570 and 1530 cm^{-1}, respectively. The parameter Δ, where $\Delta = \nu_{as}(CO_2) - \nu_s(CO_2)$, is less than that observed for NaO_2CMe (164 cm^{-1}), suggesting a bidentate bridging character for the acetate ligands [20]. The stoichiometry and the IR spectrum of this product strongly point to the structure proposed in Fig. 1, i.e. a zigzag chain obtained by axial coordination of each bridging btd ligand to two Cu^{II} ions of different dinuclear paddle-wheel units. Similar linear or zigzag $\{–Cu_2(O_2CMe)_4–L– Cu_2(O_2CMe)_4–L–\}_n$ chain structures, with L = pyrazine [21], *N*,*N*′-hexamethylenetetramine [22], dioxane [23], 2-aminopyrimidine [24], etc., have been reported in the literature. On dissolution in the good donor solvents DMF or DMSO, the polymer is broken up and the products are $[Cu_2(O_2CMe)_4(solvent)_2]$ and free btd, as deduced from single-crystal crystallography (not reported here) and IR spectroscopy of the solid copper(II) species (precipitated by addition of ether).

The possibility of preparing the dinuclear complex $[Cu_2(O_2CMe)_4(btd)_2]$ exhibiting the familiar [25] paddle-wheel cage structure was explored and realized from the reaction of $[Cu_2(O_2CMe)_4(H_2O)_2]$ with an excess (1:5, 1:7, 1:8) of btd in MeCN (Eq. (1)). The structural identity of $[Cu_2(O_2CMe)_4(btd)_2]$ (**1**) was established by single-crystal X-ray crystallography (vide infra). The large excess of btd appears absolutely necessary because otherwise, the dinuclear complex is contaminated with the above-mentioned polymeric compound, as evidenced by microanalytical data and IR spectroscopy.

$$[Cu_2(O_2CMe)_4(H_2O)_2] + 2btd \xrightarrow[\text{exc. btd}]{\text{MeCN}} \underset{\mathbf{1}}{[Cu_2(O_2CMe)_4(btd)_2]} + 2H_2O \quad (1)$$

Having obtained and identified complex **1**, the next question addressed was whether a polymeric complex could be isolated and crystallized from another solvent. However, the 1:1.4 reaction between $[Cu_2(O_2CMe)_4(H_2O)_2]$ and btd in MeOH did not yield the targeted polymeric complex with the empirical formula $Cu_2(O_2CMe)_4(btd)$. The reaction solution led to slow precipitation of well-formed crystals of the 2D polymer $\{[– btd – Cu_2(O_2CMe)_4 – btd – Cu_4(OMe)_4(O_2CMe)_2–(O_2CMe)_2–]\}_n$ (**2**), hereafter written as $\{[Cu_6(O_2CMe)_8(OMe)_4(btd)_2]\}_n$, which contains bidentate bridging btd ligands. With the identity of **2** established, an almost quantitative preparative route (not reported in Section 2) was devised by lowering the btd:Cu_2 reaction ratio from 1.4:1 to 0.7:1 (Eq. (2)):

$$3n[Cu_2(O_2CMe)_4(H_2O)_2] + 2n\,btd + 4n\,MeOH \xrightarrow{MeOH} \{[Cu_6(O_2CMe)_8(OMe)_4(btd)_2]\}n + 4n\,MeCO_2H + 6n\,H_2O \quad (2)$$

The molar ratio of the reactants in MeOH also affects the product identity. The reaction between $[Cu_2(O_2CMe)_4(H_2O)_2]$ and 5 or 7 equiv. of btd yields complex **1**, as evidenced by microanalyses and IR spectroscopy.

Since complexes **1** and **2** result from the use of different Cu_2:btd ratios, it seemed reasonable to suspect that complex **2** could be obtained by the reaction between $[Cu_2(O_2CMe)_4(H_2O)_2]$ and **1** in the appropriate molar ratio employing MeOH as solvent. The conversion of **1** to **2** can be accomplished by treatment of **1** with 2 equiv. of $[Cu_2(O_2CMe)_4(H_2O)_2]$ under reflux (Eq. (3)); this reaction has potential as a route to mixed-metal Cu^{II}/M^{II} polymers by employment of other $M_2(O_2CMe)_4$ species (e.g. M = Mo, Cr, Rh, etc.). In this reaction, the dinuclear complex **1** can be considered as a bidentate bridging "ligand" (vide infra).

$$n[Cu_2(O_2CMe)_4(btd)_2] + 2n[Cu_2(O_2CMe)_4(H_2O)_2] + 4n\,MeOH \xrightarrow[T]{MeOH} \{[Cu_6(O_2CMe)_8(OMe)_4(btd)_2]\}n + 4n\,MeCO_2H + 4n\,H_2O \quad (3)$$

3.2. Description of structures

Labelled ORTEP plots of complexes **1** and **2** are shown in Figs. 2 and 3, respectively. Selected interatomic distances and angles are collected in Tables 2 and 3, respectively.

The structure of **1** consists of centrosymmetric dinuclear $[Cu_2(O_2CMe)_4(btd)_2]$ molecules of the paddle-wheel cage type. Four *syn*,*syn* $\eta^1:\eta^1:\mu_2$ acetates bridge the two Cu^{II} atoms, while a monodentate btd ligand completes five-coordination at each metal centre. The metal coordination geometry is best described as square pyramidal with the nitrogen atom occupying the apical position. The copper(II)–oxygen distances are in the range 1.951(2)–1.972(2) Å.

The bridged dinuclear structural type $M_2(O_2CR)_4L_2$, first documented in 1953 for copper(II) acetate monohydrate [25], is ubiquitous in modern coordination chemistry. It is found not only for carboxylates of many transition elements [26], but also for dimers containing a wide variety of other triatomic bridging ligands [27]. This structural type is associated with a spectrum of metal–metal interactions [28] ranging from no interactions, weak or moderate spin-pairing in the copper(II) carboxylates, various orders of metal–metal bonding, to the "super-short" metal–metal bonds. The axial groups are normally monodentate *O*- or *N*-donors, but they may represent inter-dimer association into a polymeric structure [21–24,29,30] or may be absent [31]. Most copper(II) carboxylates exhibit the dinuclear paddle-wheel cage structure. More than 125 $[Cu_2(O_2CR)_4L_2]$ (L = monodentate *O*- or *N*-donors) structures have been reported [32,33] so far. The Cu···Cu distances in the complexes containing the CuO_4N chromophores vary from 2.58 to 2.89 Å [33,34]. Thus, the Cu(1)···Cu(1) $[-x+1, -y+1, -z+2]$ distance of 2.582(1) Å in **1** is at the lower limit of this range. Other structural features of **1** are unexceptional [34,35].

Complex **2** is a 2D coordination network. Its structure consists of tetranuclear $Cu_4(OMe)_4(O_2CMe)_4$ and dinuclear $Cu_2(O_2CMe)_4(btd)_2$ units. One dimension of the network is the polymer of the tetranuclear repeating units along the *a* axis. These polymeric chains are connected along the cell body diagonal via $Cu_2(O_2CMe)_4(btd)_2$ dimers with the btd ligands acting as the bridges between the dimers and the tetramers. Therefore, the 2D coordination network plane contains the *a* axis and the large *bc* diagonal. There are three

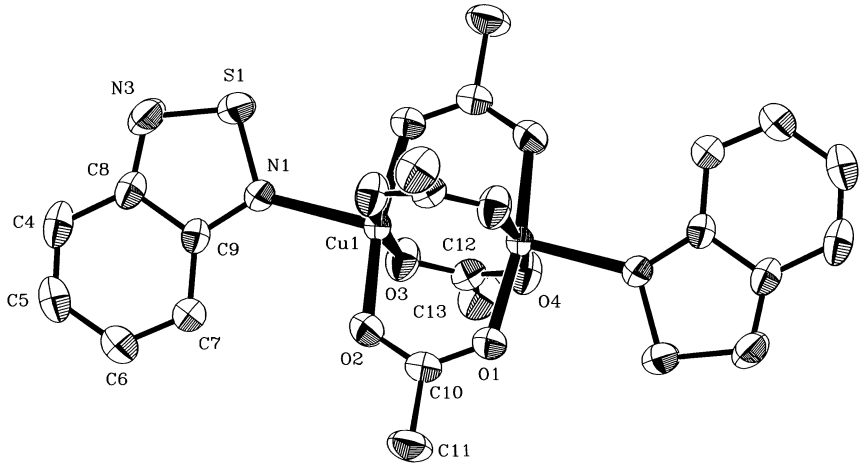

Fig. 2. The molecular structure of complex **1**; atoms generated by symmetry are not labelled.

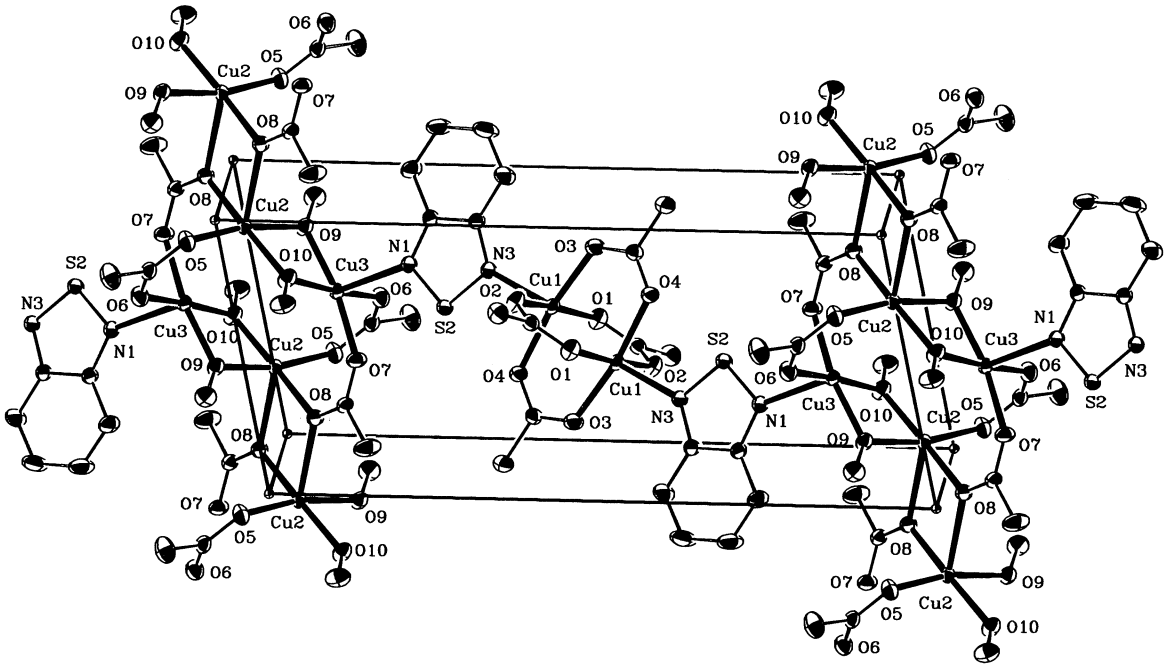

Fig. 3. ORTEP plot of the 2D network of **2**. The polymeric chains of the tetranuclear $Cu_4(OMe)_4(O_2CMe)_4$ units, developed along the *a* axis, are connected along the body diagonal via the $Cu_2(O_2CMe)_4(btd)_2$ dimers with the btd ligands acting as bridges between the dimers and the tetramers. Identical labels are used for symmetry-generated atoms.

distinct Cu···Cu separations along the *bc* diagonal chains which alternate according to the sequence …ABCABC…where (using the viewpoint of Fig. 3) A = Cu(1)···Cu(1) = 2.589(1) Å, B = Cu(1)···Cu(3) = 6.762(1) Å and C = Cu(3)···Cu(3) = 4.074(1) Å. The inter-tetramer Cu(2)···Cu(2) distance is 3.502(1) Å.

The centrosymmetric $Cu_2(O_2CMe)_4(btd)_2$ units contain four bridging acetates in the familiar $\eta^1{:}\eta^1{:}\mu_2$ coordination mode, as found in $[Cu_2(O_2CMe)_4(H_2O)_2]$ [25] and complex **1**. The Cu(1)···Cu(1) separation [2.589(1) Å] is slightly shorter than the 2.614(2) Å separation in $[Cu_2(O_2CMe)_4(H_2O)_2]$ and almost identical to that in **1**. Other bond distances and angles in the dimeric units of **2** are also very similar to those of **1**; it thus appears that these units are unperturbed. Square pyramidal coordination at the Cu(1) centres is completed by nitrogen atom N(3) of the bidentate bridging btd molecules.

The tetranuclear units sit on a crystallographic inversion centre. Within these units each Cu(2) atom is connected via two acetate bridges with one Cu(3) atom and through two methoxo bridges with the other Cu(3) atom. The acetate with oxygen atoms O(5) and O(6) is in the familiar *syn*,*syn* $\eta^1{:}\eta^1{:}\mu_2$ coordination mode and the other [that with oxygen atoms O(7) and O(8)] is in the rare $\eta^1{:}\eta^2{:}\mu_3$ mode with one O atom [O(7)] terminal to Cu(3) and the other O atom [O(8)] bridging two Cu(2) atoms belonging to different tetranuclear units. Thus, the connection of the repeating tetramers is made through their Cu(2) atoms, which are linked by two monoatomic [O(8)] bridges. The Cu(2)O(8)Cu(2)O(8) unit is strictly planar, with a crystallographic inversion centre in its middle. The intra-tetramer Cu···Cu distances are: Cu(2)···Cu(2) = 4.347(1) Å, Cu(3)···Cu(3) = 4.074(1) Å, Cu(2)···Cu(3) = 2.976(1) and 2.982(1) Å. The coordination geometry at Cu(2) and Cu(3) atoms is described as distorted square pyramidal. The apical site of the square pyramid of Cu(3) is occupied by the second nitrogen atom [N(1)] of the bridging btd ligand. Each bridging oxygen O(8) simultaneously occupies a basal site at one Cu(2) atom and the apical site of the Cu(2) atom belonging to a different tetramer. This is a common structural feature for dinuclear Cu^{II} fragments with two monoatomic bridges [36]. As a result, the two Cu(2)–O(8) distances are significantly different [1.960(2), 2.508(2) Å].

Table 2
Selected interatomic distances (Å) and angles (°) for complex **1**

Cu(1)···Cu(1a)	2.582(1)	Cu(1)–N(1)	2.214(2)
Cu(1)–O(1)	1.966(2)	N(1)–S(1)	1.617(2)
Cu(1)–O(2)	1.951(2)	C(10)–O(1)	1.248(3)
Cu(1)–O(3)	1.966(2)	C(10)–O(2a)	1.254(3)
Cu(1)–O(4)	1.972(2)		
O(1)–Cu(1)–O(2)	169.2(1)	O(2)–Cu(1)–N(1)	102.3(1)
O(1)–Cu(1)–O(3)	89.6(1)	O(3)–Cu(1)–O(4)	169.5(1)
O(1)–Cu(1)–O(4)	89.2(2)	O(3)–Cu(1)–N(1)	94.6(1)
O(1)–Cu(1)–N(1)	88.5(1)	O(4)–Cu(1)–N(1)	95.8(1)
O(2)–Cu(1)–O(3)	90.4(1)	O(2)–Cu(1)···Cu(1a)	86.5(5)
O(2)–Cu(1)–O(4)	88.8(1)	C(10)–O(1)–Cu(1)	125.0(2)

Symmetry code. a: $-x+1$, $-y+1$, $-z+2$.

Table 3
Selected interatomic distances (Å) and angles (°) for complex **2**

Cu(1)···Cu(1a)	2.589(1)	Cu(2)–O(5)	1.949(2)
Cu(1)–O(1)	1.961(2)	Cu(2)–O(8d)	2.508(2)
Cu(1)–O(2)	1.963(2)	Cu(2)–O(8b)	1.960(2)
Cu(1)–O(3)	1.957(2)	Cu(2)–O(9)	1.927(2)
Cu(1)–O(4)	1.977(2)	Cu(2)–O(10)	1.906(2)
Cu(1)–N(3)	2.227(2)	Cu(3)–O(6)	1.937(2)
Cu(1)···Cu(3)	6.762(1)	Cu(3)–O(7)	1.984(2)
Cu(2)···Cu(3)	2.976(1)	Cu(3)–O(9)	1.932(2)
Cu(2)···Cu(3b)	2.982(1)	Cu(3)–O(10)	1.908(2)
Cu(2)···Cu(2c)	3.502(1)	Cu(3)–N(1)	2.381(2)
Cu(3)···Cu(3b)	4.074(1)	Cu(2)···Cu(2b)	4.347(1)
O(1)–Cu(1)–O(2)	169.4(1)	O(8d)–Cu(2)–O(9)	99.8(1)
O(1)–Cu(1)–O(3)	90.1(1)	O(8d)–Cu(2)–O(10)	107.8(1)
O(1)–Cu(1)–O(4)	89.0(1)	O(8b)–Cu(2)–O(9)	95.9(1)
O(1)–Cu(1)–N(3)	95.3(1)	O(8b)–Cu(2)–O(10)	171.3(1)
O(2)–Cu(1)–O(3)	89.7(1)	O(9)–Cu(2)–O(10)	76.5(1)
O(2)–Cu(1)–O(4)	89.3(1)	O(6)–Cu(3)–O(7)	93.4(1)
O(2)–Cu(1)–N(3)	95.1(1)	O(6)–Cu(3)–O(9)	96.0(1)
O(3)–Cu(1)–O(4)	169.4(1)	O(6)–Cu(3)–O(10)	171.7(1)
O(3)–Cu(1)–N(3)	102.5(1)	O(6)–Cu(3)–N(1)	91.2(1)
O(4)–Cu(1)–N(3)	88.1(1)	O(7)–Cu(3)–O(9)	168.8(1)
O(5)–Cu(2)–O(8d)	89.2(1)	O(7)–Cu(3)–O(10)	93.9(1)
O(5)–Cu(2)–O(8b)	93.2(1)	O(7)–Cu(3)–N(1)	82.1(1)
O(5)–Cu(2)–O(9)	168.4(1)	O(9)–Cu(3)–O(10)	76.3(1)
O(5)–Cu(2)–O(10)	93.8(1)	O(9)–Cu(3)–N(1)	103.8(1)
O(8d)–Cu(2)–O(8b)	77.5(1)	Cu(2)–O(9)–Cu(3)	100.9(1)
		Cu(2)–O(10)–Cu(3)	102.6(1)

Symmetry codes: a: $-x+1$, $-y+1$, $-z+1$; b: $-x+1$, $-y$, $-z+2$; c: $-x$, $-y$, $-z+2$; d: $x-1$, y, z.

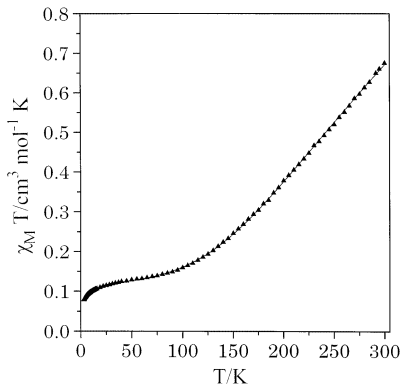

Fig. 4. Plot of $\chi_M T$ versus T for complex **2**; χ_M is the molar magnetic susceptibility per six Cu^{II} ions. The solid line represents the best fit according to Eq. (4) (see Section 3.4).

The 2D structure of **2** can be described as being composed of $\{[Cu_4(OMe)_4(O_2CMe)_4]\}_n$ chains "bridged" by $Cu_2(O_2CMe)_4(btd)_2$ units. The conversion of $[Cu_2(O_2CMe)_4(btd)_2]$ (**1**) to **2** is thus quite understandable.

The closest precedent to **2** is the 2D polymer $\{[Cu_4(O_2CMe)_8(bppz)]\}_n$, where bppz is the bis-bidentate bridging ligand 2,5-bis(2-pyridyl)pyrazine [37]. Its structure consists of $\{[Cu_2(syn,syn\ \eta^1{:}\eta^1{:}\mu_2\text{-}O_2CMe)_2(bppz)]^{2+}\}_n$ chains "bridged" by $Cu_2(syn,syn\ \eta^1{:}\eta^1{:}\mu_2\text{-}O_2CMe)_4(syn,anti\ \eta^1{:}\eta^1{:}\mu_2\text{-}O_2CMe)_2^{2-}$ units. Also of relevance are the 1D polymers $\{[Cu_4(O_2CMe)_8(bpy)_2]\}_n$ [36] and $\{[Cu_4(O_2CMe)_8(amp)_2]\}_n$ [38] that contain two distinct types of Cu_2^{4+} units, each lying on a crystallographic inversion centre [bpy = 2,2′-bipyridine and amp = 2-(aminomethyl)pyridine]. The chains are formed by alternating $Cu_2(O_2CMe)_4$ and $Cu_2(O_2CMe)_2(bpy)_2^{2+}$ or $Cu_2(O_2CMe)_2(amp)_2^{2+}$ units connected by *syn*,*anti* bridging acetate groups; the $Cu_2(O_2CMe)_4$ unit has the classic tetra-bridged, paddle-wheel structure with two oxygens from the two *syn*,*anti* acetates occupying the axial positions.

Complexes **1** and **2** join a handful of structurally characterized coordination compounds of btd [39]. In all the reported structures btd behaves as a bidentate bridging ligand; thus, complex **1** is the first complex in which btd adopts a monodentate coordination mode.

3.3. IR spectroscopy

The IR spectra of complexes **1** and **2** exhibit the typical bands of the disubstituted benzene ring, bands assignable to vibrations of the thiadiazole ring and the characteristic bands of the acetate ligands. The bands at 1438 (**1**), 1455 (**2**) and 830 (**1**), 864 (**2**) are associated with the ν(CN) and ν(SN) vibrational modes of the thiadiazole ring [40], respectively. Due to coordination, these bands are shifted compared to those in free btd [15].

The spectra exhibit the antisymmetric and symmetric carboxylate stretching vibrations at 1554 (**1**), 1576 (**2**) and 1404 (**1**), 1426 (**2**), respectively. The values of Δ, where $\Delta = \nu_{as}(CO_2) - \nu_s(CO_2)$, are less than the value observed for NaO_2CMe (164 cm^{-1}), as expected for the bridging mode of carboxylate ligation in **1** and **2** [20].

The medium intensity band of **1** at 1024 cm^{-1} is assigned to the C–O stretching vibration of the bridging methoxo group [1g,41].

3.4. Magnetic and EPR studies of complex *2*

Variable-temperature (3–300 K) magnetic susceptibility data were collected for a polycrystalline sample of the polymeric complex. The temperature dependence of the product $\chi_M T$, where χ_M is the molar magnetic susceptibility per Cu_6^{II} and T is the absolute temperature, is shown in Fig. 4. The room temperature value of $\chi_M T$ (0.675 cm^3 K mol^{-1}) is much smaller than that expected for six uncoupled $S = 1/2$ spins (2.225 cm^3 K mol^{-1}), indicative of strong antiferromagnetic coupling even at room temperature. The $\chi_M T$ product decreases rapidly with decreasing temperature down to approximately 100 K and less between 100 and 25 K; it starts to decrease rapidly again below 25 K, reaching the value of 0.078 cm^3 K mol^{-1} at 3 K. The continuous

decrease of $\chi_M T$ upon cooling down is also in line with antiferromagnetic exchange interactions.

Obviously no exact treatment can be made for the determination of the various exchange interactions in the 2D polymer **2**. In an attempt to probe deeper into the superexchange interactions, the magnetic behaviour of the complex is closely combined with its molecular and crystal structure. It was previously shown that **2** consists of 1D chains—in which the repeating unit is a planar copper(II) tetramer (part A)—interconnected by paddle-wheel $Cu_2(O_2CMe)_4$ units (part B) through the bidentate bridging btd ligands. Consequently, we could easily detect at least three different J values; these interactions are schematically shown in Fig. 5, in which, for clarity, the copper(II) numbering scheme is different compared with that used in Fig. 3. The magnetic exchange interactions inside each tetranuclear unit Cu(1)Cu(2)Cu(3)Cu(4) are expressed by J_1 and J_2, while

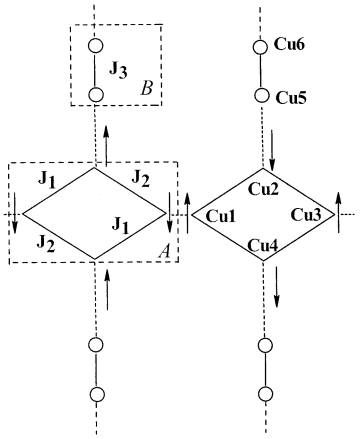

Fig. 5. The model used to interpret the magnetic properties of the 2D coordination polymer **2**. Fragment (part A) represents the planar tetranuclear unit and fragment B the dinuclear unit. Two neighbouring tetranuclear units and two dinuclear units are drawn. The exchange parameters J_1, J_2 and J_3 are clarified in the left tetranuclear and dinuclear units (those inside the dashed boxes), while the copper(II) numbering scheme used in the magnetic study is shown in the right units. The direction of the spins in the chain consisting of repeating tetranuclear units is also shown. The correspondence between the copper(II) numbering scheme used in the structural section with that in the magnetic one is as follows: Cu(1) = Cu(5), Cu(1) = Cu(6), Cu(2) = Cu(3), Cu(2) = Cu(1), Cu(3) = Cu(2) and Cu(3) = Cu(4).

Table 4
Expressions for the energy levels of states deduced from the Hamiltonian expressed by Eq. (5) [a]

$S=2$	$E=-J_1-J_2$
$S=1$	$E=J_1-J_2$
$S=1$	$E=-J_1+J_2$
$S=1$	$E=J_1+J_2$
$S=0$	$E=J_1+J_2+2(J_1^2+J_2^2-J_1J_2)^{1/2}$
$S=0$	$E=J_1+J_2-2(J_1^2+J_2^2-J_1J_2)^{1/2}$

[a] See text.

J_3 represents the interaction within each dinuclear unit Cu(5)Cu(6). Due to the large Cu(5)···Cu(2) distance [6.762(1) Å, this corresponds to the Cu(1)···Cu(3) distance in the real structure], we could assume that there is no interaction between parts A and B. Moreover, due to the relatively large Cu(3)···Cu(3) and Cu(1)···Cu(1) distances [3.502(1) Å, these correspond to the Cu(2)···Cu(2) distance in the real structure], the interaction between two neighbouring tetranuclear units along the chain could be modelled by a mean field correction.

The composite nature of **2** permits the magnetic susceptibility to be modelled as the sum of the individual intramolecular susceptibilities (Eq. (4)):

$$\chi_M = \chi_A + \chi_B + 6N\alpha \quad (4)$$

where χ_A stands for the Bleaney–Bowers equation and χ_B is the susceptibility of the tetranuclear unit (Eq. (5)) with a mean field correction, θ, the other symbols having their usual meanings.

$$X_B = \frac{2Ng^2\beta^2}{3k(T-\theta)} \frac{\sum_i S_i(S_i+1)(2S_i+1)e^{-E_i/KT}}{\sum_i (2S_i+1)e^{-E_1/KT}} \quad (5)$$

The Hamiltonian of the tetranuclear model is

$$H = -2J_1(S_1S_2 + S_3S_4) - 2J_2(S_2S_3 + S_4S_1) \quad (6)$$

where the diagonal interactions are negligible; its eigenvalues can be easily derived and are given in Table 4. The best fitting parameters obtained are $J_1 = -80(5)$ cm^{-1}, $J_2 = -240(6)$ cm^{-1}, $J_3 = -210(8)$ cm^{-1}, $g = 2.23(3)$, $\theta = -0.53(1)$ K and $R = 4.23 \times 10^{-6}$, where $R = \Sigma[(\chi_M)_{calc} - (\chi_M)_{obs}]^2$. The excellent fit is shown in Fig. 4. Moreover, although more than one g parameter has been used to fit the magnetic data in other 2D polymers [37], only one was used here to avoid overparametrization. The J trend thus obtained will be discussed in the next section. It should be emphasized again that the above magnetic model (Eq. (4)) for **2**, is an approximation only.

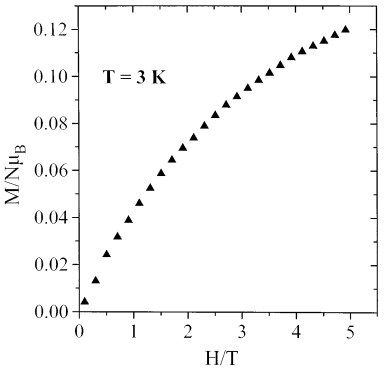

Fig. 6. Magnetization isotherm plot at 3 K from 0 to 5 T for complex **2**.

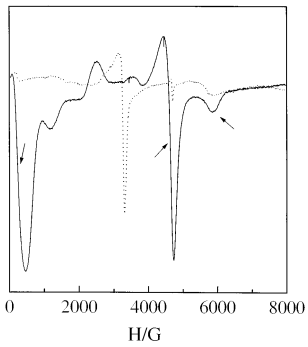

Fig. 7. X-band EPR spectra of the polycrystalline powder of **2** at room temperature (solid line) and at 4 K (dotted line); the arrows show the position of the partially resolved triplet spectrum.

The molar magnetization data recorded at 3 K in the magnetic field range 0–5 T are shown in Fig. 6. The curve is far from saturation at maximum field (0.12 μ_B at 5 T), indicating very weak interchain or interplane antiferromagnetic interactions [37].

The room temperature X-band EPR spectrum of a powdered sample of complex **2**, shown in Fig. 7 (solid line), exhibits many features in the 30–6000 G field range. The set of bands at 246 (H_{z1}), 4636 ($H_{\perp 2}$) and 5872 (H_{z2}) G could be attributed to a well resolved triplet with axial symmetry and relatively high D value. By assuming $E = 0$, the parameters are $D = 0.341(5)$ cm^{-1}, $g_z = 2.38(1)$ and $g_{x,y} = 2.08(3)$. These values compare well with those of previously reported tetraacetatodicopper(II) systems [31,32]. A second set of bands at ca. 1214, 2536 and 3750 G overlaps with the former, corresponding to the higher states of the tetranuclear unit in the chain populated at room temperature. The powder spectrum of **2** at 4 K is also shown in Fig. 7 (dotted line). It is clear that the intensity of the triplet signals has been decreased considerably, denoting the depopulation of the triplet state of the tetraacetatodicopper(II) system. The second set of bands vanishes at 4 K, indicating that the $S = 0$ state is populated in the tetranuclear unit at this low temperature. The feature at 3300 G can be attributed to paramagnetic impurities.

3.5. Orbital interpretation of the exchange mechanism

Despite the lack of an appropriate theoretical magnetic model to fit the data, a 3-J model was constructed within the framework of this study. Its construction was based upon the structural characteristics of complex **2**; however, some assumptions were made. These assumptions are examined first. In the following parts of our discussion, we mainly adopt the numbering scheme of Fig. 3; in some cases, however, the numbering scheme of Fig. 5 will also be given in square brackets for clarity.

It was assumed that the superexchange interactions between the tetranuclear and dinuclear units is negligible. Actually, the structure of **2** clearly shows that both Cu(1) ions of the dinuclear unit are in square pyramidal environments. This, along with the long axial Cu(1)–N(3) distances [2.227(2) Å], suggest that the unpaired electron at each Cu(1) magnetic centre is described by a $x^2 - y^2$-type magnetic orbital pointing from the metal towards the four nearest neighbouring donor atoms, O(1), O(2), O(3) and O(4). Thus, there is no spin density on the N(3) atoms coming from Cu(1). This should also be the case with the spin density on the N(1) atoms coming from Cu(3) ions, since these ions are also in square pyramidal environments and the axial Cu(3)–N(1) distances are long [2.381(2) Å]. All these could well account for the lack of exchange interactions between Cu(1) and Cu(3) [between parts A and B in Fig. 5], propagated through the bridging btd ligand, verifying the first assumption made in the construction of the model.

The second assumption made was that the intertetranuclear interaction (along the chain of tetranuclear units) could be modelled by a mean field correction. The tetranuclear units are connected along their chains via two long Cu(2)–O(8) bonds [2.508 Å]. In particular, each Cu(2) ion is in a distorted square pyramidal environment and its four-nearest neighbouring donor atoms are O(5), O(8), O(9) and O(10), lying at the basal plane; still another bridging O(8) atom, belonging to the Cu(2) basal plane of the neighbouring tetranuclear unit, occupies its apex at a distance of 2.508(2) Å. Again, there is no spin density on the apical O(8) atom coming from Cu(2) at 2.508 (2) Å, verifying the second assumption made in the construction of the 3-J magnetic model.

The J-trend derived, $J_2 > J_3 > J_1$, is examined next. J_1 corresponds to the exchange interactions within the Cu(2)(η^1:η^1:μ_2-O_2CMe)(η^1:η^2:μ_3-O_2CMe)Cu(3) dinuclear subunit, J_2 to the interactions within the dialkoxo-bridged copper(II) subunit Cu(2)(μ-OMe)$_2$Cu(3), and J_3 to the interactions within the quadruply-bridged tetraacetatodicopper(II) $Cu_2(\eta^1{:}\eta^1{:}\mu_2\text{-}O_2CMe)_4$ unit. From literature it is well known that (a) complexes containing the $[Cu_2(syn,syn\ \eta^1{:}\eta^1{:}\mu_2\text{-}O_2CR)_2]^{2+}$ core are characterized by antiferromagnetic interactions with the singlet–triplet energy gap values ($-2J$) in the range 86–125 cm^{-1} [42], (b) the $-2J$ values of the dialkoxo-bridged roof-shaped copper(II) dimers are in the 0.6–168 cm^{-1} range [1h], and (c) complexes $[Cu_2(\eta^1{:}\eta^1{:}\mu_2\text{-}O_2CR)_4L_2]$ with a cage structure exhibit antiferromagnetic interactions with the $-2J$ values ranging between 224 and 555 cm^{-1} [31,42]. Based upon these literature reports, a probable J-trend might be $J_3 > J_2 \approx J_1$. However, the experimental relationship observed is $J_2 > J_3 > J_1$. Since the two acetate bridges propagate a weaker interaction than that of the four

ones [42], the lowest J_1 value of -80 cm^{-1} ($-2J_1 =$ 160 cm^{-1}) among the three derived, could be accepted for the bis(acetato)dicopper(II) core. The reason for the greater J_2 value is investigated next.

The dialkoxo bridged Cu(2)(μ-OMe)$_2$Cu(3) subunit found in **2** is a symmetrical roof-shaped moiety, since it possesses four almost equal Cu–O bonds [two pairs of 1.906(2) and 1.927(2) Å], a mean Cu(2)–O–Cu(3) angle (φ_{mean}) value of 101.7° [two φ values of 100.9(1) and 102.6(1)°] and a dihedral O(9)Cu(2)O(10)/O(9)Cu(3)O(10) angle, ω, of 161.6°. Our groups have established a magneto-structural correlation [1h], holding for symmetrical roof-shaped, dialkoxo-bridged Cu(OR)$_2$Cu moieties. A comparison between the Cu–O bond length, φ and ω structural parameters of the Cu(OR)$_2$Cu moiety of **2** and those presented in Ref. [1h], clearly shows that the former (i) is a symmetrical dialkoxo-bridged Cu(II) moiety, (ii) exhibits the second highest φ_{mean} value, (iii) has the shortest tetrad of Cu–O bonds, and (iv) possesses an ω value between the two extreme values (176.3 and 150.8°) observed so far. Consequently, based upon its φ_{mean} and ω values, this is arranged in the antiferromagnetic region of the contour plot with the sharper plot [43]. However, the sharper the slope, the stronger the antiferromagnetic interaction. This, along with the short Cu–O bond lengths, could well account for the very high J_2 value (-240 cm^{-1}) derived. To the best of our knowledge, complex **2** has the highest $-J$ value ever derived for a symmetrical, roof-shaped Cu(OR)$_2$Cu moiety.

For paddle-wheel complexes of the formula [Cu$_2$(O$_2$CR)$_4$L$_2$] (L = monodentate ligand) the exchange interaction between the two d^9 Cu^{II} ions is strongly antiferromagnetic, because unpaired electron density from both metal ions is transferred to the same orbital of the bridging carboxylate ligand [31,32,44]. Although these complexes have very short Cu···Cu distances (2.58–2.89 Å) [34], the $-2J$ values (224–555 cm^{-1} [42]) are known to be relatively insensitive to this parameter [44]. The main factors which determine the magnitude of the antiferromagnetic interaction is the electronic structure of the bridging OCO moiety and the bending of the Cu–O–C–O–Cu bridge, the latter being measured by the dihedral angle, φ_{bend}, between the CuOOCu mean plane and the carboxylate moiety. In particular, the singlet–triplet separation ($-2J$) depends upon [31,32,42,44,45] the electron donating ability of the R substituent of the carboxylate bridging ligand, the σ-donor ability of the axial ligand, the planarity of the basal planes at the Cu^{II} centres, the dihedral angle between the two metal-containing basal planes and the bending of the Cu–O–C–O–Cu bridge. Despite being lower than J_2 value [$-240(6)$ cm^{-1}], J_3 is particularly high in this category. For example, the $-2J$ values of [Cu$_2$(O$_2$CMe)$_4$(py)$_2$] [45], [Cu$_2$(O$_2$CMe)$_4$(α-pic)$_2$] [35], [Cu$_2$(O$_2$CMe)$_4$(β-pic)$_2$] [35] and [Cu$_2$(O$_2$CMe)$_4$(γ-pic)$_2$] [35] are 333, 332, 326 and 333 cm^{-1}, respectively, while the $-2J$ value calculated for the dinuclear tetraacetate moiety of **2** is 420 cm^{-1} (py = pyridine, α-pic = 2-methylpyridine, β-pic = 3-methylpyridine and γ-pic = 4-methylpyridine). The high J_3 value could be attributed to the small displacement of the Cu(1) ions [Cu(5) and Cu(6) in Fig. 5] from their basal planes (0.18 Å), the non-significant variation of the Cu(1)–O–C angles [ranging from 120.5(2) to 125.0(2)°], the zero dihedral angle between the two Cu^{II}-containing basal planes and the almost zero values [$\varphi_{bend.\ Cu(1)O(3)O(4)Cu(1)/C(12)O(3)O(4)} = 0.16°$, $\varphi_{bend.\ Cu(1)O(1)O(2)Cu(1)/C(10)O(1)O(2)} = 0.5°$] of the dihedral angles between the CuOOCu and bridging OCO planes; the fourth parameter is very important because a relatively large, i.e. 7–11° [32,44], bending of the Cu–O–C–O–Cu bridges would lead to a decrease of $-2J$ due to reduced overlap between the copper(II) $d_{x^2-y^2}$ orbital and the $2p_x$ carboxylate oxygen orbital in the symmetric HOMO [32,44,46].

4. Conclusions

The [Cu$_2$(O$_2$CMe)$_4$(H$_2$O)$_2$]/btd reaction system fulfilled its promise as a source of interesting complexes. The present work has given one dinuclear tetracarboxylate-bridged complex with the familiar paddle-wheel cage structure and one 2D polymeric species possessing unusual structural features. The former has two free coordination sites and acts as bidentate bridging ligand for the construction of the latter. The structures of the products of this reaction system emphasize the capabilities of btd to behave both as a terminal and a bridging ligand and of the carboxylate group to adopt a number of different ligation modes, including μ_2 and μ_3 ones. This suggests a rich source of untapped chemistry with the btd-RCO$_2^-$ ligands' "blend" for the preparation of novel high nuclearity and polymeric compounds of other 3d metals, and further studies are in progress. Magnetochemical data of the 2D coordination polymer clearly show antiferromagnetic exchange interactions between the copper(II) ions.

5. Supplementary material

Crystallographic data (excluding structure factors) in CIF format for the structural analysis have been deposited with the Cambridge Crystallographic Data Centre, CCDC Nos. 163549 (**1**) and 163550 (**2**). Copies of this information may be obtained free of charge from The Director, CCDC, 12 Union Road, Cambridge CB2 1EZ, UK (fax: +44-1223-336-033; e-mail: deposit@ccdc.cam.ac.uk or www: http://www.ccdc.cam.ac.uk).

Acknowledgements

The authors gratefully acknowledge the Greek General Secretariat of Research and Technology (Grant 99ED139 to V.P.) for support of this work.

References

[1] (a) G.S. Papaefstathiou, S.P. Perlepes, A. Escuer, R. Vicente, M. Font-Bardia, X. Solans, Angew. Chem., Int. Ed. 40 (2001) 884;
(b) G.S. Papaefstathiou, C.P. Raptopoulou, A. Tsohos, A. Terzis, E.G. Bakalbassis, S.P. Perlepes, Inorg. Chem. 39 (2000) 4658;
(c) V. Tangoulis, C.P. Raptopoulou, V. Psycharis, A. Terzis, K. Skorda, S.P. Perlepes, O. Cador, O. Kahn, E.G. Bakalbassis, Inorg. Chem. 39 (2000) 2522;
(d) A. Tsohos, S. Dionyssopoulou, C.P. Raptopoulou, A. Terzis, E.G. Bakalbassis, S.P. Perlepes, Angew. Chem., Int. Ed. 38 (1999) 983;
(e) V. Tangoulis, C.P. Raptopoulou, A. Terzis, E.G. Bakalbassis, E. Diamantopoulou, S.P. Perlepes, Inorg. Chem. 37 (1998) 3142;
(f) V. Tangoulis, C.P. Raptopoulou, S. Paschalidou, E.G. Bakalbassis, S.P. Perlepes, A. Terzis, Angew. Chem., Int. Ed. Engl. 36 (1997) 1083;
(g) V. Tangoulis, C.P. Raptopoulou, S. Paschalidou, A.E. Tsohos, E.G. Bakalbassis, A. Terzis, S.P. Perlepes, Inorg. Chem. 36 (1997) 5270;
(h) V. Tangoulis, C.P. Raptopoulou, A. Terzis, S. Paschalidou, S.P. Perlepes, E.G. Bakalbassis, Inorg. Chem. 36 (1997) 3996;
(i) A. Panagiotopoulos, T.F. Zafiropoulos, S.P. Perlepes, E. Bakalbassis, I. Masson-Ramade, O. Kahn, A. Terzis, C.P. Raptopoulou, Inorg. Chem. 34 (1995) 4918.
[2] (a) D. Gatteschi, Phil. Trans. R. Soc. London A 357 (1999) 3079;
(b) O. Kahn, Molecular Magnetism, Wiley-VCH, New York, 1993.
[3] J.S. Miller, Phil. Trans. R. Soc. London A 357 (1999) 3159 and references therein.
[4] O. Kahn, Acc. Chem. Res. 33 (2000) 647.
[5] G. Christou, D. Gatteschi, D.N. Hendrikson, R. Sessoli, MRS Bull. 25 (2000) 1.
[6] H.O. Stumpf, L. Quahab, Y. Pei, P. Bergerat, O. Kahn, J. Am. Chem. Soc. 116 (1994) 3866.
[7] J.L. Manson, A.M. Arif, J.S. Miller, Chem. Commun. (1999) 1479.
[8] (a) N. Masciocchi, P. Cairati, L. Carlucci, G. Menza, G. Cianni, A. Sironi, J. Chem. Soc., Dalton Trans. (1996) 2739 and references therein;
(b) Y.-S. Zhang, G.D. Enright, S.R. Breeze, S. Wang, New J. Chem. 23 (1999) 625;
(c) S. Subramanian, M.J. Zaworotko, Angew. Chem., Int. Ed. Engl. 34 (1995) 2127;
(d) A.J. Blake, N.R. Champness, A.N. Khlobystov, D.A. Lemenovskii, W.-S. Li, M. Schröder, Chem. Commun. (1997) 1339;
(e) F. Lloret, G. De Munno, M. Julve, J. Cano, R. Ruiz, A. Caneschi, Angew. Chem., Int. Ed. 37 (1998) 135;
(f) M.A. Lawandy, X. Huang, R.-J. Wang, J. Li, J.Y. Lu, T. Yuen, C.L. Lin, Inorg. Chem. 38 (1999) 5410;
(g) R.D. Bailey, W.T. Pennington, Polyhedron 16 (1997) 417;
(h) P. Jensen, S.R. Batten, G.D. Fallon, D.C.R. Hockless, B. Moubaraki, K.S. Murray, R. Robson, J. Solid State Chem. 145 (1999) 387.
[9] W. Kobel, M. Hanack, Inorg. Chem. 25 (1986) 103.
[10] O. Jung, C.G. Pierpont, J. Am. Chem. Soc. 116 (1994) 2229.
[11] M. Fujita, Y.J. Kwon, S. Washizu, K. Ogura, J. Am. Chem. Soc. 116 (1994) 1151.
[12] A.J. Blake, N.R. Brooks, N.R. Champness, P.A. Cooke, A.M. Deveson, D. Fenske, P. Hubberstey, W.-S. Li, M. Schröder, J. Chem. Soc., Dalton Trans. (1999) 2103.
[13] M. Munakata, L.P. Wu, T. Kuroda-Sowa, Bull. Chem. Soc. Jpn. 70 (1997) 1727.
[14] G.S. Papaefstathiou, A. Tsohos, C.P. Raptopoulou, A. Terzis, V. Psycharis, D. Gatteschi, S.P. Perlepes, Cryst. Growth Design 1 (2001) 191.
[15] G.S. Papaefstathiou, S.P. Perlepes, A. Escuer, R. Vicente, A. Gantis, C.P. Raptopoulou, A. Tsohos, V. Psycharis, A. Terzis, E.G. Bakalbassis, J. Solid State Chem. 159 (2001) 371.
[16] V. Luzzati, Acta Crystallogr. 4 (1951) 193.
[17] A.I. Vogel, A Text-Book of Quantitative Inorganic Analysis, 3rd ed., Longman, London, 1969, p. 497.
[18] G.M. Sheldrick, SHELXS 86, Structure Solving Program, University of Göttingen, Göttingen, Germany, 1986.
[19] G.M. Sheldrick, SHELXL 93, Program for Crystal Structure Refinement, University of Göttingen, Göttingen, Germany, 1993.
[20] G.B. Deacon, R.J. Phillips, Coord. Chem. Rev. 33 (1980) 227.
[21] (a) J.S. Valentine, A.J. Silverstein, Z.G. Soos, J. Am. Chem. Soc. 96 (1974) 97;
(b) B. Morosin, R.C. Hughes, Z.G. Soos, Acta Crystallogr., Sect. B 31 (1975) 762.
[22] J. Pickardt, Acta Crystallogr., Sect. B 37 (1981) 1573.
[23] M.M. Borel, A. Leclaire, Acta Crystallogr., Sect. B 32 (1976) 1275.
[24] G. Smith, C.H.L. Kennard, K.A. Byriel, Polyhedron 10 (1991) 873.
[25] J.N. van Nieker, F.R.L. Schoening, Acta Crystallogr. 6 (1953) 227.
[26] For a tabulation see: Y.B. Koh, G.C. Christoph, Inorg. Chem. 18 (1979) 1122.
[27] F.A. Cotton, R.A. Walton, Multiple Bonds Between Metal Atoms, Wiley, New York, 1982.
[28] L.C. Porter, M.H. Dickman, R.J. Doedens, Inorg. Chem. 22 (1983) 1962 and references cited therein.
[29] E. Melnik, Coord. Chem. Rev. 42 (1982) 259.
[30] R.H. Cayton, M.H. Chisholm, J.C. Huffman, E.B. Lobkovsky, J. Am. Chem. Soc. 113 (1991) 8709 and references cited therein.
[31] M. Kato, Y. Muto, Coord. Chem. Rev. 92 (1988) 45.
[32] F.P.W. Agterberg, H.A.J.P. Kluit, W.L. Driessen, J. Reedijk, H. Oevering, W. Buijs, N. Veldman, M.T. Lakin, A.L. Spek, Inorg. Chim. Acta 267 (1998) 183.
[33] M. Ghassemzadeh, K. Aghapoor, B. Neumüller, Z. Naturforsch., Teil b 53 (1998) 774.
[34] M.R. Sundberg, R. Uggla, M. Melnik, Polyhedron 15 (1996) 1157.
[35] M. Yamanaka, H. Uekusa, S. Ohba, Y. Saito, S. Iwata, M. Kato, T. Tokii, Y. Muto, O.W. Steward, Acta Crystallogr., Sect. B 47 (1991) 344.
[36] S.P. Perlepes, E. Libby, W.E. Streib, K. Folting, G. Christou, Polyhedron 11 (1992) 923.
[37] A. Neels, H. Stoeckli-Evans, A. Escuer, R. Vicente, Inorg. Chem. 34 (1995) 1946.
[38] C.A. Crawford, E.F. Day, W.E. Streib, J.C. Huffman, G. Christou, Polyhedron 13 (1994) 2933.
[39] (a) M. Munakata, T. Kuroda-Sowa, M. Maekawa, M. Nakamura, S. Akiyama, S. Kitagawa, Inorg. Chem. 33 (1994) 1284;
(b) M.W. Renner, K.M. Barkigia, D. Melamed, K.M. Smith, J. Fager, Inorg. Chem. 35 (1996) 5120.
[40] A.A. El-Azhary, Spectrochim. Acta A 52 (1996) 33.
[41] L.A.P.M. Hall, Polyhedron 9 (1990) 2575.
[42] K. Geetha, A.R. Chakravarty, J. Chem. Soc., Dalton Trans. (1999) 1623 and references cited therein.

[43] See figure 9 of Ref. [1h].
[44] F.P.W. Agterberg, H.A.J.P. Kluit, W.L. Driessen, H. Oevering, W. Buijs, M.T. Lakin, A.L. Spek, J. Reedijk, Inorg. Chem. 36 (1997) 4321.
[45] S. Ohba, M. Kato, T. Tokii, Y. Muto, O.W. Steward, Mol. Cryst. Liq. Cryst. 233 (1993) 335.
[46] T. Kawata, H. Uekusa, S. Ohba, T. Furukawa, T. Tokii, Y. Muto, M. Kato, Acta Crystallogr., Sect. B 48 (1992) 253.